



25<sup>th</sup> ABCM International Congress of Mechanical Engineering  
October 20-25, 2019, Uberlândia, MG, Brazil

**COB-2019-0978**

## **NONLINEAR ANALYSES OF STEEL PLATES SUBMITTED TO AXIAL COMPRESSION FORCES CONSIDERING RESIDUAL STRESSES**

**Elvys Dias Reis**

**Caroline Martins Calisto**

**Ana Lydia Reis de Castro e Silva**

**Hermes Carvalho**

Federal University of Minas Gerais, Department of Structural Engineering, Belo Horizonte – MG, Brazil.

e-mails: elvysdiasreis@gmail.com, carolinemartinscalisto@yahoo.com.br, analydiarcs@gmail.com, hermes@dees.ufmg.br.

**Abstract.** *This study evaluates the steel plates' behavior exclusively subjected to axial compressive forces due to static actions considering initial imperfection and residual stresses. Linear analyses of plate stability were performed with variations in the boundary conditions to obtain the values of the critical buckling load and the main buckling modes. For this, numerical models were developed in the Abaqus, commercial software for analyses, and it made it possible to study the variation in the value of the elastic buckling coefficient as a function of the ratio between the lengths of the plate sides through the critical buckling load. Considering the initial imperfection and distribution of residual stresses of plates cut with a blowtorch in both longitudinal edges, the principal approach of this work is the plate behavior subject to nonlinear analysis. The results of the elastic buckling coefficient obtained in the numerical analyses converged to the values found in the literature, which validates the use of the proposed models. The values of the ultimate buckling load of plates cut with blowtorch obtained through nonlinear analyses were lower than those obtained by the buckling analyses, which shows the influence of the initial imperfection and the residual stresses.*

**Keywords:** *compressed steel plates, residual stresses, numerical modeling, nonlinear analyses.*

### **1. INTRODUCTION**

According to Fakury *et al.* (2016), steel structural elements are designed to withstand tensile and compressive stresses, since they behave very well under these two stresses. In this paper, however, only the behavior of steel plates and bars subjected exclusively to axial compressive forces resulting from static actions will be evaluated.

In this aspect, it was studied the procedures for buckling analyses of some isolated steel plates. The linearized stability analysis for plates with some variations in the boundary conditions was performed, obtaining the values of the buckling critical load and the predominant buckling modes.

It is important to emphasize that some important aspects of the numerical analysis were evaluated, such as the mesh sensitivity, the introduction of residual stresses, the consideration of elastic-plastic material and the behavioral coherence of the plate in the cases studied. In the case of nonlinear analyses, it is noted that the plate is long, with a large ratio between the sides, which prevents the interference of the constraint in the region near the loaded edge and enables to verify the behavior of the plates with dimensions normally used in the composition of structural profiles.

It is also known that plates and profiles present geometric imperfections (initial curvature) due to the manufacturing process, transportation, and storage. Thus, as the load is imposed, this imperfection increases and, consequently, the bending moment acting in the plate central section or profile becomes more accentuated. Another consequence of the parts manufacturing process is the appearance of residual stresses, which can accelerate the collapse process by leading the parts to premature yielding in regions where the residual stresses are of compression. These factors affect the plates' strength and metal bars, leading them to lose stiffness more quickly.

According to Castro e Silva (2006), a slender elastic plate does not collapse soon after buckling but can withstand loads significantly higher than its critical load without deforming excessively. In this phenomenon, called post-buckling resistance, Fakury *et al.* (2016) show that the profile, composed of plates subject to local buckling, tends to maintain its straight longitudinal axis, while the compressed elements of its cross-section buckle according to a succession of longitudinal half-waves with equal lengths. As the plate evolves in the post-buckling path, the transversal fibers become tensile, opposing the increase in deformation and leading the profile to withstand forces beyond the critical buckling load.

Numerical models were developed in Abaqus, commercial software for analyses that works with the finite element method (Dassault Systèmes, 2013). Specifically, the variation in the value of the elastic buckling coefficient,  $K_q$ , as a

function of  $a:b$  ratio (side lengths) was studied from the analysis of critical buckling loads and mainly the influence of imperfection and the introduction of residual stresses in the behavior of the plate. The analyses were nonlinear and considered the distribution of residual stresses of plates cut with a blowtorch in both longitudinal edges. The results obtained in the numerical analyses were compared with theoretical and literature values, presented by Castro and Silva (2006), Bradford and Azhari (1997) and Reddy (1999).

## 2. METHODOLOGY

In the compressed bars (plates) design, one of the failure modes to be considered is the bar instability, assumed with initial curvature. The other collapse mode is the local buckling of the component elements of the cross-section of the plate, such as the buckling of the web or the flanges of section I or H (Fakury *et al.*, 2016).

Thus, it is necessary to make a study about plates behavior submitted to axial forces of compression, considering, among other factors, the influence ratio between the plate lengths in obtaining the critical buckling load.

### 2.1 Compressed steel plates

As in the study of Castro and Silva (2006), for the linearized stability analyses of isolated plates, this study considers a plate with  $a:b$  ratio between sides (being in the longitudinal direction) submitted to uniform uniaxial compression, as shown in Fig. 1. It was assumed that the plate has a constant thickness and isotropic material. Furthermore, it is perfectly flat, elastic, without residual stresses and loaded exactly in its middle plane.

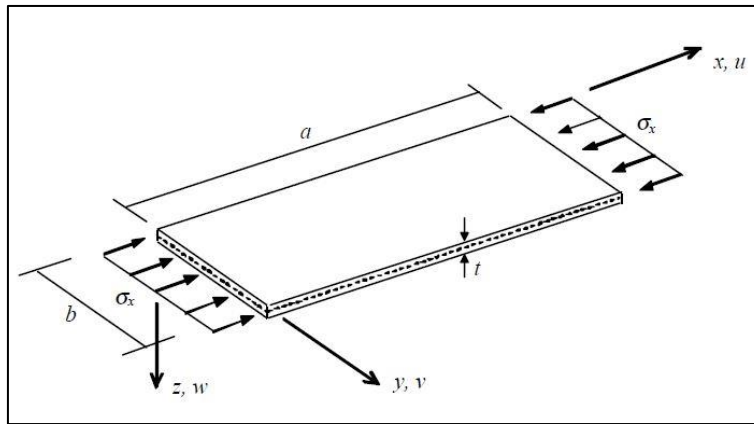


Figure 1. Uniaxially compressed plate (Castro and Silva, 2006).

Under these conditions, according to Ugural (1981), by establishing appropriate boundary conditions, the elastic buckling stress ( $\sigma_{cr}$ ) is reached through of Eq. (1).

$$\sigma_{cr} = K_q \frac{\pi^2 E}{12(1-\nu^2)} \left(\frac{t}{b}\right)^2 \quad (1)$$

Where  $E$  is the longitudinal modulus of the material,  $t$  is the plate thickness,  $\nu$  is the Poisson coefficient,  $b$  is the plate width and  $K_q$  is the plate buckling coefficient, given by Eq. (2).

$$K_q = \left(\frac{mb}{na} + \frac{na}{mb}\right)^2 \quad (2)$$

Since  $a$  is the length of the longitudinal edge discharged,  $b$  is the length of the transversal edge loaded,  $n$  the number of half-waves that appear in the transversal direction of  $\sigma_x$ , taken equal to 1, and  $m$  the number of half-waves that appear during buckling in the direction of  $\sigma_x$ . According to Trahair and Bradford (1988) and Salmon and Johnson (1990), for  $m = 1, 2, 3, 4$ , etc,  $K_q$  values are obtained as a function of the relation between the plate sides ( $a:b$ ).

Fig. 2 shows, for example, that in the case of plates with simply supported longitudinal edges, the  $K_q$  value tends to a minimum value equal to 4, as the  $a:b$  ratio increases, regardless of the loaded edges constraint type.

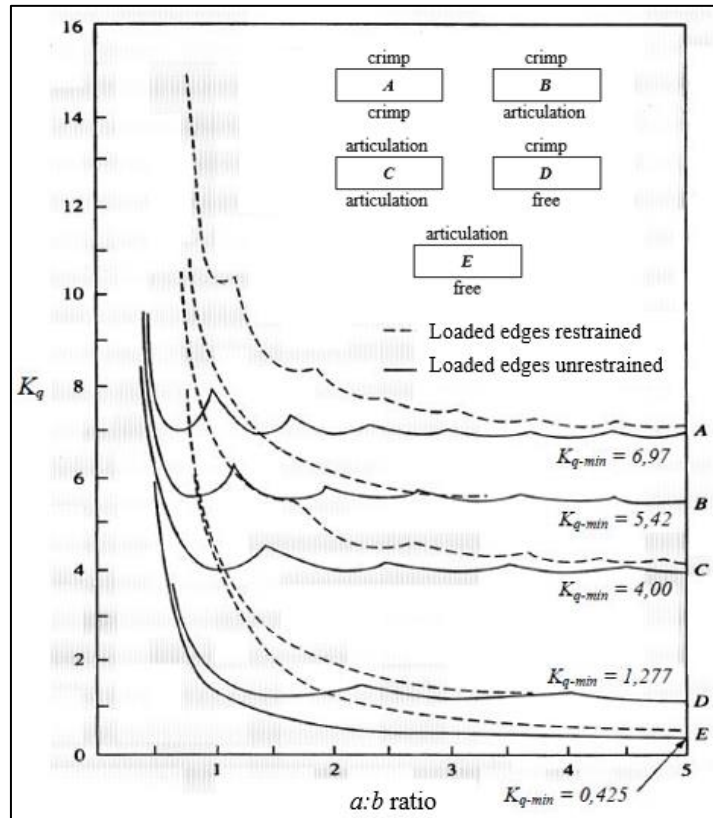


Figure 2.  $K_q$  values for the usual types of plate boundary conditions (Salmon and Johnson, 1990).

Local buckling is characterized by the first buckling mode (critical mode). Thus, the numerical analysis is used to obtain the critical buckling stresses (eigenvalues) and the eigenvector corresponding to the critical mode.

The numerical modeling of the plate under axial compressive stress allows obtaining the eigenvalues ( $\lambda$ ) of the problem, with which the critical elastic buckling load ( $q_{cr}$ ) is reached by multiplying it by the applied axial compressive load ( $q$ ), usually unitary, according to Eq. (3).

$$q_{cr} = \lambda q \quad (3)$$

With the plate thickness ( $t$ ) and the critical elastic buckling load ( $q_{cr}$ ), the critical stress ( $\sigma_{cr}$ ), previously unknown, is reached by Eq. (4).

$$\sigma_{cr} = \frac{q}{t} \quad (4)$$

Once the critical stress ( $\sigma_{cr}$ ) is obtained and with the other parameters mentioned above, the elastic buckling coefficient of the plate ( $K_q$ ) is calculated using the Eq. (1).

## 2.2 Laminated plates

According to Castro and Silva (2006), in laminated plates, the distribution of average residual longitudinal stresses, taken in the cross-sectional skeleton line, should be parabolic with compression at the edges and tension at the center, as shown in Fig. 3. As the equilibrium of the longitudinal forces must be guaranteed, the parabolic consideration requires that the compressive stresses ( $\sigma_c$ ) at the plate edges are double (in absolute value) the tensile stress ( $\sigma_t$ ) of the middle of the plate. Besides, two parameters that affect the value of the residual stresses in the plates are the slenderness, corresponding to the relation between the width and the thickness ( $b/t$ ), and the perimeter ratio for the cross-sectional area ( $\alpha$ ).

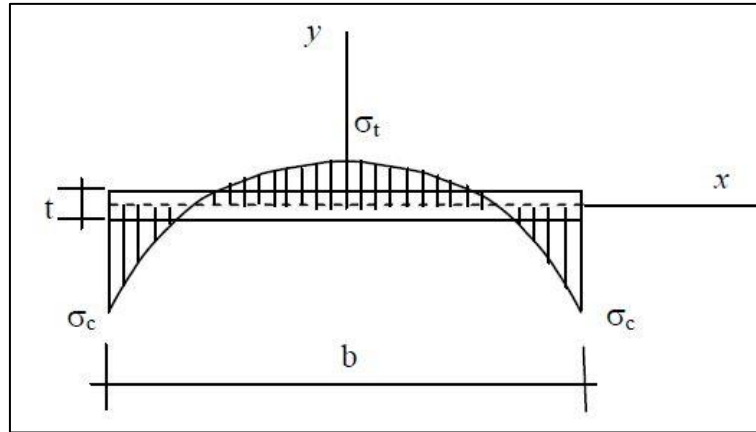


Figure 3. Parabolic distribution of residual stresses in laminated slabs (Castro e Silva, 2006).

The residual stress distribution of laminated plates, proposed by Alpsten (1972), is obtained by Eq. (5).

$$\alpha = \frac{2(b+t)}{bt} \quad (5a)$$

$$\sigma_c = \frac{0,18}{\alpha^{3/2}} \left( \frac{b}{t} \right) \quad (5b)$$

$$\sigma_c = \frac{\sigma_c}{2} \quad (5c)$$

### 2.3 Plates cut with a blowtorch

For a plate cut with a blowtorch in both longitudinal edges, the residual stress distribution has the pattern shown in Fig. 4.

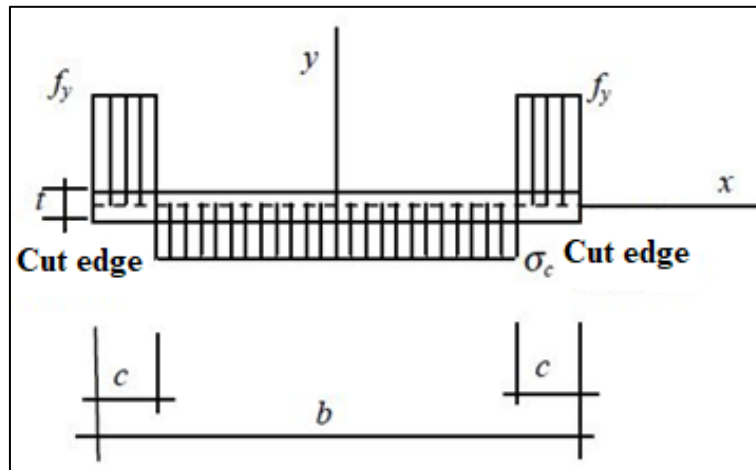


Figure 4. Distribution of residual stresses in slabs cut at both edges.

The uniform residual longitudinal stress,  $\sigma_c$ , is given by Eq. (6).

$$\sigma_c = f_y \frac{2c}{(b-2c)} \quad (6)$$

From an experimental study of residual stresses in steel plates cut with a blowtorch on one edge, with thickness and yield stress ( $f_y$ ) in MN/mm<sup>2</sup>, Young and Dwight (1971) obtained the width of the tensile rectangle ( $c$ ), in mm, given by Eq. (7).

$$c = \frac{1100 \sqrt{t}}{f_y} \quad (7)$$

## 2.4 Numerical modeling

In numerical modeling, for geometrically nonlinear structures is chosen the static analysis that adopts the Linear Arc Length technique, proposed by Riks (1972). Also, the elastic-plastic behavior is perfect and it was considered in all analyses the longitudinal elasticity modulus is equal to  $200 \times 10^9$  Pa and the Poisson coefficient is equal to 0.3.

Moreover, the mesh convergence and sensitivity tests are performed to know the influence of its discretization on the value of the coefficient  $K_q$ . To do this, the 0.002 m thick board, with sides equal to 0.200 m, loaded (transversal) edges simply supported and discharged (longitudinal) edges will be analyzed. The result of the convergence test obtained for this case will be adopted for the others in all the analyses.

After the numerical analyses, the values of the coefficient  $K_q$  that refer to the critical tension of the first mode of buckling are obtained. The process is repeated for different meshes and then the curve is plotted with the number of divisions of the mesh versus the coefficient  $K_q$ , to verify the convergence of the results.

Finally, after performing the nonlinear analyses of the element, it is possible to extract from Abaqus software a coefficient of proportionality to be applied in the critical buckling load referring to the first mode of buckling ( $q_{cr}$ ). This coefficient is called Load Proportionality Factor (*LPF*) and its use is expressed in Eq. (8).

$$q_{ult} = LPF \cdot q_{cr} \quad (8)$$

## 3. RESULTS AND DISCUSSIONS

It was studied the variation in the value of the  $K_q$  coefficient as a function of the a:b ratio through analysis to obtain a critical buckling load and the plate behavior through nonlinear analysis, considering the distribution of residual stresses of plates cut with a blowtorch in both longitudinal edges. Before, however, the modeling parameters were defined through a convergence and sensitivity test.

### 3.1 Convergence and sensitivity test

Several finite mesh elements were tested to obtain the eigenvalue corresponding to the first mode of buckling presented by the plate. According to Trahair and Bradford (1988) and Salmon and Johnson (1990), the value of the coefficient  $K_q$  for uniaxially compressed plates with cantilever unloaded edges, supported edges and *a:b* ratio equal to 1.0, the theoretical value of  $K_q$  is about 7.8.

After numerical obtaining the theoretical value and the eigenvalue, the presented methodology was carried out for meshes with several configurations and the results of the numerical analyses converged to a value of  $K_q$  close to 7.7 with the mesh refinement, as shown in Fig. 5.

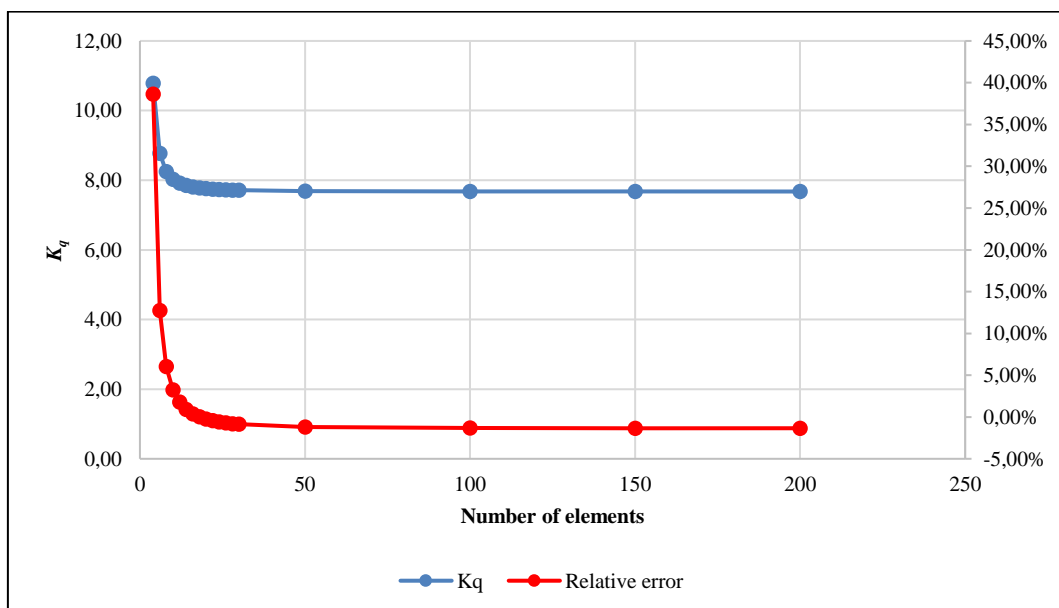


Figure 5. Results of the mesh convergence and sensitivity test.

It was also observed that the relative error becomes insignificant from a given moment, and it is possible to adopt a mesh with good sensitivity to the behavior expected by the part when it is subjected to the axial compression load. It was chosen, therefore, by the mesh of 20 elements in each direction, corresponding to the overall length of each element equal to 0.010 m.

### 3.2 Relationship between $K_q$ and a:b ratio

With the results of the mesh convergence and sensitivity test, the same analysis was also performed for cases in which the plate sides are different, i.e., when the a:b ratio becomes different from 1, according to the results presented in Tab. 1 and Fig. 6. In Case 1 there are cantilever edges and supported edges and in Case 2 there are only cantilever edges.

Table 1.  $K_q$  results by numerical analyses for Cases 1 and 2.

a:b	q [N/mm]	$\lambda$ (Abaqus)		$q_{cr}$ [N/mm]		$\sigma_{cr}$ [N/mm <sup>2</sup> ]		$K_q$	
		Case 1	Case 2	Case 1	Case 2	Case 1	Case 2	Case 1	Case 2
1	1	281	369	281	369	140	185	7,76	10,21
2	1	254	287	254	287	127	143	7,01	7,94
3	1	257	268	257	268	128	134	7,1	7,41
4	1	254	262	254	262	127	131	7,01	7,26
5	1	255	259	255	259	127	129	7,04	7,16
6	1	254	257	254	257	127	129	7,01	7,12
7	1	254	256	254	256	127	128	7,03	7,09
8	1	254	256	254	256	127	128	7,01	7,07

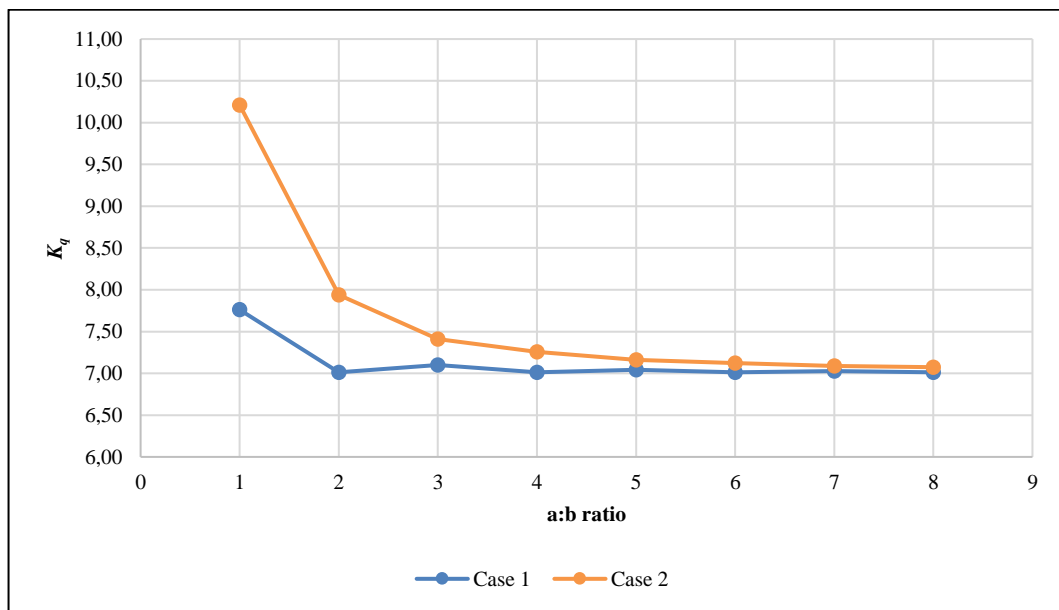


Figure 6. Variation of  $K_q$  with a:b ratio for Cases 1 and 2.

When comparing the curves proposed by Salmon and Johnson (1990), which shows  $K_q$  values for the usual types of plate contour conditions with the results obtained numerically some important observations can be highlighted: the value of  $K_q$  when there are cantilever edges are always larger than when there are supported edges; by increasing the a:b ratio the value of the buckling coefficient decreases in both cases; from a certain point, with the increase of the relation a:b,  $K_q$  has a value close to 7.0 (Case 1). Then the boundary conditions of the longitudinal edges do not interfere significantly in the part behavior.

It was also noted that the values obtained numerically were very close to the values in the literature, presented by Castro and Silva (2006), Bradford and Azhari (1997) and Reddy (1999), according to Tab. 2. The comparison between these values and those obtained numerically validates the use of the proposed models.

Table 2.  $K_q$  values from numerical analyses and literature.

a:b	$K_q$ (Abaqus)	$K_q$ (Castro e Silva)	$K_q$ (Bradford e Azhari)
1	7,76	7,69	7,69
2	7,01	7,02	6,99
3	7,10	7,11	7,42
4	7,01	7,02	-
5	7,04	7,05	-
6	7,01	7,02	-
7	7,03	7,04	-
8	7,01	7,03	-

### 3.3 Introduction of residual stresses

For a plate cut with a blowtorch in both longitudinal edges, with a:b ratio equal to 8, the residual stresses to be applied to the plate were obtained. These stresses were applied in the mesh rows, respecting the stress distribution proposed by Alpsten (1972). The eigenvalue for the first buckling mode was obtained, equal to 113.00, which, when multiplied by the load of 1,000 N/m, according to Eq. (3), leads to the critical buckling load that it will be used in the nonlinear analysis, performed next. Fig. 7 shows the plate deformed configuration when the residual stresses increase.

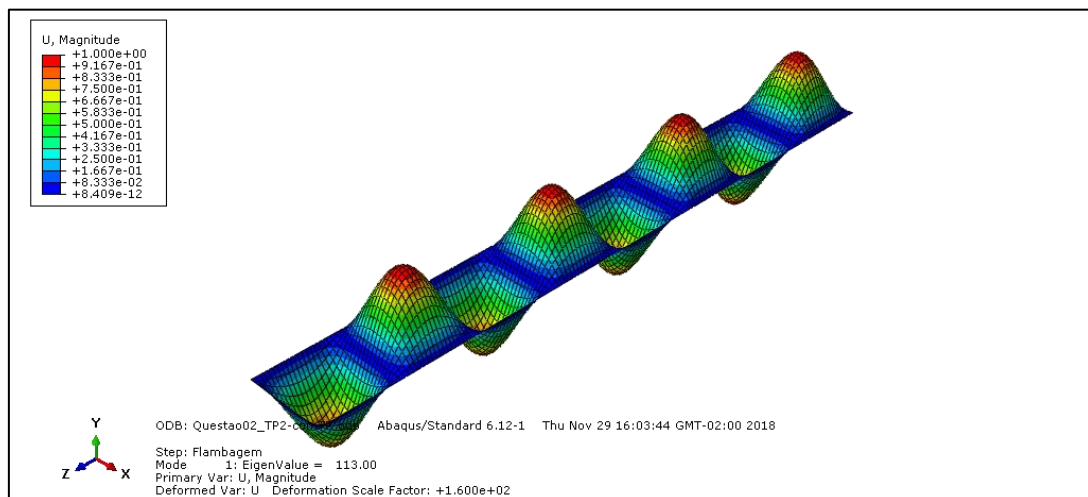


Figure 7. Deformed plate with increased residual stresses.

From the model configuration presented in Fig. 7, it is noted that there are eight points in which the strain is maximum, four in which it is positive and four in which it is negative. Thus, the central point of the third half-wave (from left to right) was chosen, referring to node 1061 of the element, and an initial imperfection corresponding to 10% of the plate thickness was added to it, i.e., 0.2 mm.

After a nonlinear analysis of Riks, by the complete integration of type S4, the model led to an *LPF* of 2.08, which multiplied by the above-mentioned critical buckling load, according to Eq. (8), leads to a critical load of 234,860 N/m, corresponding to a negative vertical displacement of 0.00445 m.

The plate vertical displacement increases as the load is increased and decreases after the ultimate load is reached, due to consideration of the perfect elastic-plastic behavior. This phenomenon can be better understood from the graph shown in Fig. 8, in which the red curve refers to the displacements after reaching the ultimate load (in this figure, the values refer to the displacement module).

Note that the value obtained by nonlinear analysis, considering residual stresses and initial imperfections of approximately 235,000 N/m, is lower than that obtained by buckling analysis, equal to 254,000 N/m. This occurs because, for this case the residual stresses are high and high values of compressive stresses are observed for a plate long section, which makes the collapse earlier.

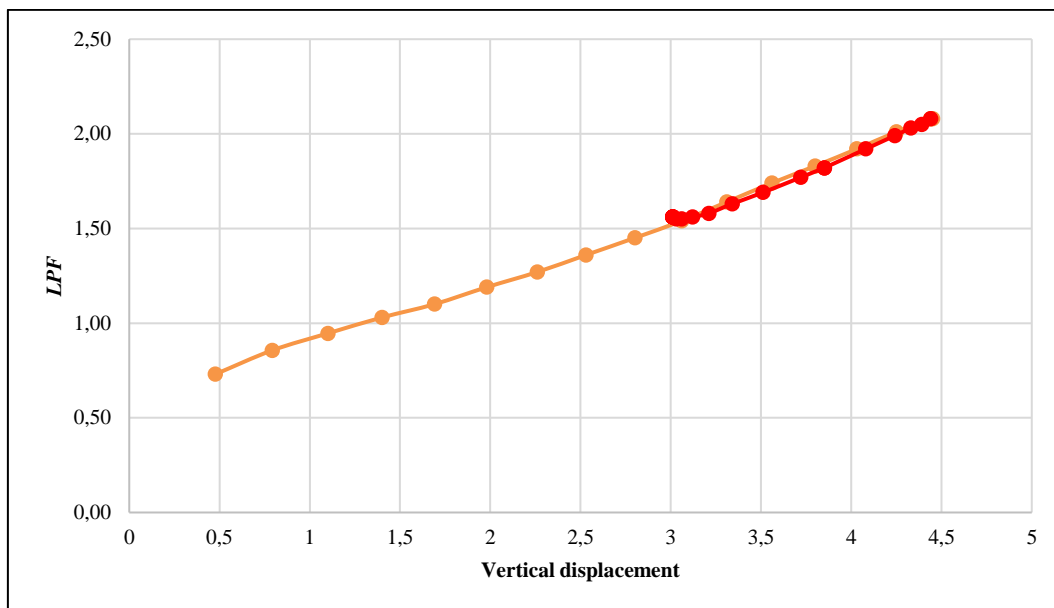


Figure 8. Displacement variation with *LPF*.

#### 4. CONCLUSIONS

The phenomenon of uniaxially compressed plates local buckling was analyzed in this study and the results obtained were compared numerically with the theoretical values found in the literature. It was also studied the influence of the initial imperfection and introduction of residual stresses in the behavior of the plates.

For uniaxially compressed plates, the mesh convergence and sensitivity test were performed, from which the mesh utilization was determined with 20 elements in each direction, that is, the overall length of 0.01 m of each element.

The variation in the value of the coefficient  $K_q$  as a function of  $a:b$  ratio (sides lengths) was studied by critical buckling load analysis for two cases, differentiated only by the boundary conditions. The results pointed to the buckling coefficient decrease while the  $a:b$  ratio was increased, which converged to values found in the literature, a situation in which the constraint conditions of the longitudinal edges no longer interfere in the behavior of the parts.

Finally, the plate behavior was studied and the ultimate buckling load was obtained by nonlinear analysis, considering the distribution of residual stresses of plates cut with a blowtorch in both longitudinal edges. It was observed that the outcomes obtained by the nonlinear analysis, considering still initial imperfection, are lower than those obtained by the buckling analysis, what happened because in plates cut with blowtorch the residual stresses are high and high values of compressive stresses are observed over a long section, which makes the collapse earlier.

#### 5. ACKNOWLEDGEMENTS

The authors would like to acknowledge the financial support from the Brazilian Council of Research (CNPq) and Minas Gerais Research Foundation (FAPEMIG).

#### 6. REFERENCES

- Alpsten, G., 1972. *Prediction of thermal residual stresses in hot-rolled plates and shapes of structural steel*. Swedish Institute of Steel Construction.
- Bradford, M.A. and Azhari, M., 1997. "The use of bubble functions for the stability of plates with different end conditions". *Engineering Structures*, Vol. 19, No. 2, pp. 151-161.
- Castro e Silva, A.L.R., 2006. *Análise numérica não-linear da flambagem local de perfis de aço estrutural submetidos à compressão uniaxial*. Ph.D. thesis, Federal University of Minas Gerais, Belo Horizonte, Brazil.
- Dassault Systèmes, 2013. *Abaqus 6.13 Online Documentation*.
- Fakury, R.H.; Castro e Silva, A.L.R.; Caldas, R.B., 2016. *Dimensionamento de elementos estruturais de aço e mistos de aço e concreto*. Pearson Education do Brasil. São Paulo.
- Reddy, J.N., 1999. "Theory and analysis of elastic plates. Taylor & Francis.

- Riks, E., 1972. “The application of Newton’s method to the problem of elastic stability”. *Transactions of the ASME: Journal of Applied Mechanics*.
- Salmon, C.G. and Johnson, J.E., 1990. *Steel structures: Design and behaviour: Emphasizing load and resistance factor design*. 3<sup>a</sup> ed., Harper Collins Publishers Inc.
- Trahair, N.S. and Bradford, M.A., 1988. *The behavior and design of steel structures*. 2<sup>a</sup> ed., Chapman & Hall.
- Ugural, A.C., 1981. *Stresses in plates and shells*. McGraw-Hill.
- Young, B.W. and Dwight, J.B. (1971). *Residual stresses and their effect on the momentcurvature properties of structural steel sections*. CIRIA Tech, Note 32.

## **7. RESPONSIBILITY NOTICE**

The authors are the only responsible for the printed material included in this paper.